

Measurement of the analyzing power for n-p radiative capture

J. P. Soderstrum* and L. D. Knutson

University of Wisconsin, Madison, Wisconsin 53706

(Received 9 January 1987)

A beam of polarized neutrons has been used to measure the analyzing power for n-p radiative capture at a lab angle of 90° and neutron energies of 6.0 and 13.43 MeV. Both reaction products were detected with good energy resolution, and time-of-flight techniques were used to remove unwanted background. The measured analyzing powers are consistent with the results of deuteron photodisintegration experiments in which the polarization of the outgoing neutron is measured. The results are somewhat less negative than currently available theoretical calculations which include meson-exchange currents.

I. INTRODUCTION

It has recently been suggested^{1,2} that there may be a discrepancy between theory and experiment for the polarization of neutrons (p_n) from deuteron photodisintegration at $\theta_{c.m.} = 90^\circ$. A number of groups^{1,3-5} have reported measurements of p_n for photon energies between 6 and 14 MeV, and over this range the data tend to be somewhat less negative than classical impulse calculations such as those of Partovi.⁶ Since the neutron polarization arises mainly from $E1$ - $M1$ interference terms involving $M1$ spin-flip transitions, one expects that the measurements will be sensitive to the presence of meson exchange currents. According to calculations reported by Hadjimichael⁷ and by Arenhovel *et al.*⁸ (the latter at $\theta_{c.m.} = 60^\circ$), meson exchange currents do produce a significant change in p_n , but the effect is to move the theoretical curve to more negative values, thus making the discrepancy between theory and experiment even more pronounced.^{1,2}

Although these results suggest that the current theoretical description of deuteron photodisintegration may be lacking in some respects, one should not rule out the possibility that the experiments are in error. Measurements of this kind are quite difficult to obtain, and the results reported by various groups do not agree in all cases. In view of these concerns, and in view of the importance of understanding the two-nucleon system, it is clear that additional experimental work on this problem would be of value.

In the present experiment, a beam of polarized neutrons has been used to measure the analyzing power (which is proportional to the left-right asymmetry in the yield of gamma rays) at 90° for n-p radiative capture. By time-reversal invariance, this is equivalent to measuring the polarization of the neutrons from deuteron photodisintegration. Measurements have been obtained at neutron lab energies of 6.0 and 13.43 MeV, corresponding to $E_\gamma = 5.24$ and 9.00 MeV for the inverse reaction.

Section II contains a discussion of the experimental arrangement. In Sec. III we outline the data reduction procedures and describe the calculation of multiple scattering and finite geometry corrections. The final results and conclusions are given in Sec. IV.

II. EXPERIMENTAL DETAILS

The main experimental difficulties are brought on by the fact that the cross section for n-p capture is very small (about $4 \mu\text{b}/\text{sr}$), while the cross section for n-p elastic scattering is on the order of $100 \text{ mb}/\text{sr}$. It is not trivial to distinguish between the two types of events, because both produce one charged particle and one neutral particle. However, if one detects both reaction products with good energy resolution and makes use of time-of-flight information, it is possible to eliminate the unwanted background.

A schematic diagram of the experimental setup is shown in Fig. 1. A beam of polarized charged particles (protons or deuterons) is incident on a 10.5 cm long neutron production cell which contains either tritium or deuterium gas at a pressure of approximately 700 Torr. Polarized neutrons emerging from the cell at $\theta \approx 0^\circ$ interact in a cylindrical container of NE213 liquid scintillator (H/C ratio = 1.213), located 50 cm (center to center) from the production cell. The liquid scintillator, which is 6.6 cm in diameter and 15 cm high, serves to detect the recoil deuterons. Gamma rays from n-p capture in the liquid are detected in a 25.4 cm diam by 25.4 cm long NaI crystal, located 77 cm (center to center) from the target at $\theta_{\text{lab}} = 90^\circ$. Borated paraffin is used to shield the NaI crystal against direct neutrons from the production cell. The NaI detector is surrounded by a 3 cm thick layer of $^6\text{Li}_2\text{CO}_3$, which absorbs thermal neutrons, and by approximately 10 cm of lead. A plastic scintillator anticoincidence detector is used to reject cosmic rays and events in which Compton-scattered or 511 keV gamma rays escape from the crystal.

The polarized neutrons were produced by the reactions $^3\text{H}(\vec{p}, \vec{n})^3\text{He}$ at $E_n = 6.0$ MeV, and $^2\text{H}(\vec{d}, \vec{n})^3\text{He}$ at $E_n = 13.43$ MeV. Vector-polarized proton and deuteron beams were obtained from the University of Wisconsin crossed-beams polarized ion source,⁹ accelerated by a tandem Van de Graaff accelerator, and then focused on the neutron production cell. Because of count rate considerations, beam currents on target were limited to 50–60 nA for protons and 16–17 nA for deuterons. With these beam currents the singles rates in the detectors were

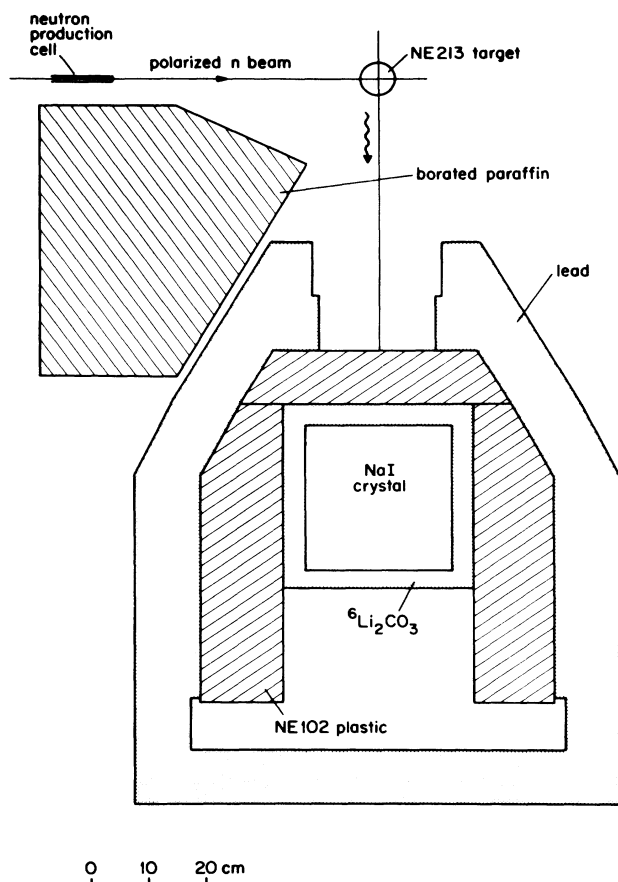


FIG. 1. Experimental setup.

roughly 50–75 kHz for the liquid scintillator and 2 kHz for the NaI.

The polarization of the neutrons was determined by measuring the polarization of the charged particle beam and making use of the known polarization transfer coefficients.^{10,11} The beam polarization was measured periodically (typically once per day) with an accurately calibrated proton¹² or deuteron¹³ polarimeter located on a separate beamline. In addition, a transmission polarimeter¹⁴ located in the beamline between the analyzing magnet and the production cell was used to monitor the polarization at more frequent intervals. The polarization was stable to within the statistics of the measurement during each running period. Typical neutron polarizations were 0.73 at $E_n=6.0$ MeV and 0.54 at $E_n=13.43$ MeV. The sign of the charged particle beam polarization was reversed every 0.25 sec by switching rf transitions at the ion source. This also reverses the sign of the neutron polarization. The difference in magnitude of the polarization between the two spin states was typically less than 0.01.

A considerable amount of effort went into optimizing the energy resolution of the liquid scintillator. In the final design the cell consisted of a cylindrical Pyrex container wrapped with Teflon tape and viewed at each end by a photomultiplier tube. The typical resolution for the

recoil deuterons was about 16% full width at half maximum (FWHM). The typical resolution of the NaI detector was about 6% FWHM. Additional details concerning the performance of the NaI detector are given in Ref. 15.

Since the coincidence rate between the two detectors was not large, all valid coincidence events were accepted into an on-line computer and stored event by event on magnetic tape for later analysis. A fast, 200 nsec wide overlap between timing signals from the liquid scintillator and the NaI detector was used to enable a time-to-amplitude converter for the time-of-flight (TOF) measurement and to gate signals into analog-to-digital converters. The fast overlap also enabled a pulse shape discrimination (PSD) circuit (similar to that of Ref. 16) which was used to distinguish between neutron- and gamma-induced events in the liquid scintillator. A pile-up reject circuit was used to eliminate events in which two pulses occurred in the liquid scintillator within 600 nsec of each other. This ensures that the crossover of the bipolar signal in the PSD circuit will be clean. For each valid event energy signals from the liquid scintillator and NaI detector were accepted into the computer along with the outputs from the TOF and PSD circuits. The total event rate into the computer was approximately 30 Hz, of which approximately 8 per hour were true n-p capture events.

To determine the dead time in the circuit a pulser (referred to as the LT pulser), triggered at a rate proportional to the charged particle flux on the neutron production cell, was introduced into both detectors immediately after the phototubes and allowed to propagate through the entire circuitry into the computer. The dead time, which arises primarily from the pile-up reject circuit, was typically 15–20%.

To determine the integrated neutron flux on the NE213 target, a second pulser (referred to as the IC pulser) was introduced into the NaI electronics. By determining the number of pulses in coincidence with high-energy neutron-induced events in the target, we obtain a good measure of the relative number of neutrons incident on the scintillator for each spin state. Further experimental details are given in Ref. 17.

III. DATA REDUCTION AND ANALYSIS

A. Identification of the n-p capture events

Samples of the raw data accepted into the computer at $E_n=6.0$ and 13.43 MeV are shown in Figs. 2 and 3, respectively. In the PSD spectra one sees separate peaks from gamma- and neutron-induced events. The TOF spectra consist of a prominent peak corresponding to prompt gamma rays and a flat background which arises from random coincidences. The width of the peak is about 3 nsec FWHM. The energy scale in the E_{NaI} spectra can be established from peaks at $E_\gamma=4.44$ MeV [from $^{12}\text{C}(n,n'\gamma)$] and at 6.79 MeV (from thermal neutron capture on ^{127}I). The only distinctive feature in the NE213 spectrum is the edge which corresponds to n-p elastic scattering at 180°. Since the light response of the liquid scintillator is quite nonlinear with energy, particularly at low energies, the NE213 spectra shown are also nonlinear.

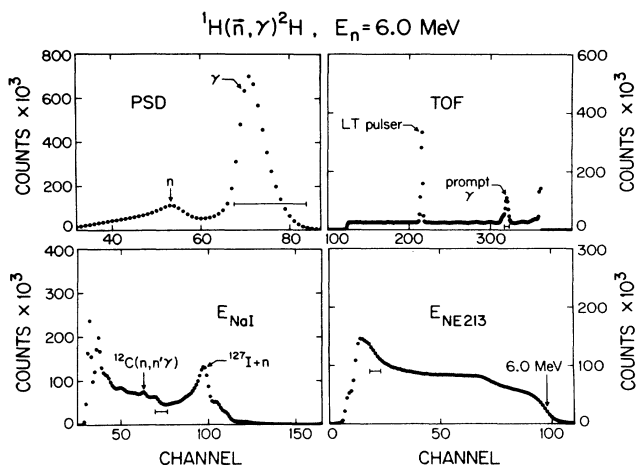


FIG. 2. Typical spectra showing raw data (with no cuts) at $E_n=6.0$ MeV. All events must satisfy a 200 nsec coincidence condition between the two detectors. The positions of the windows which optimize the yield of real events, as explained in the text, are indicated.

To remove unwanted events from these spectra, software cuts were made on each of the four signals. The initial step was to place windows around the neutron peak in the PSD spectrum and the prompt gamma ray peak in the TOF spectrum. With these conditions imposed, it is possible to see an isolated peak at the expected point in the two-dimensional E_{NaI} vs E_{NE213} spectrum. Once the peak has been located, we construct a set of four one-dimensional spectra which contain only good events. In each spectrum we include only those events for which the three remaining parameters fall within the appropriate windows. The capture peak is then seen clearly in each spectrum, and this makes it possible to optimize the position and width of each window. The final windows are marked in Figs. 2 and 3.

Note that the PSD windows are not symmetric about the neutron peaks. In the raw spectra most of the counts

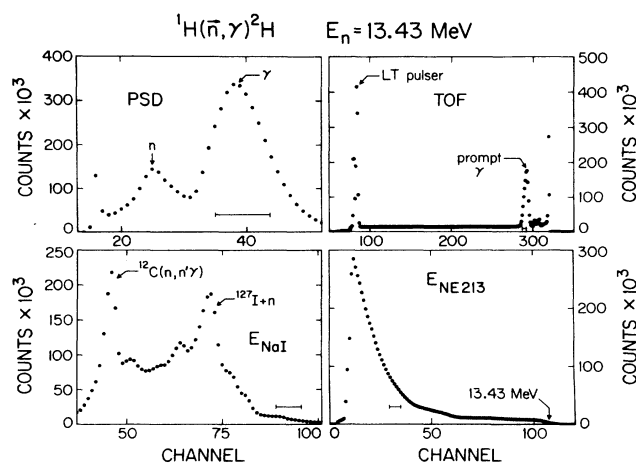


FIG. 3. The same as Fig. 2 at $E_n=13.43$ MeV.

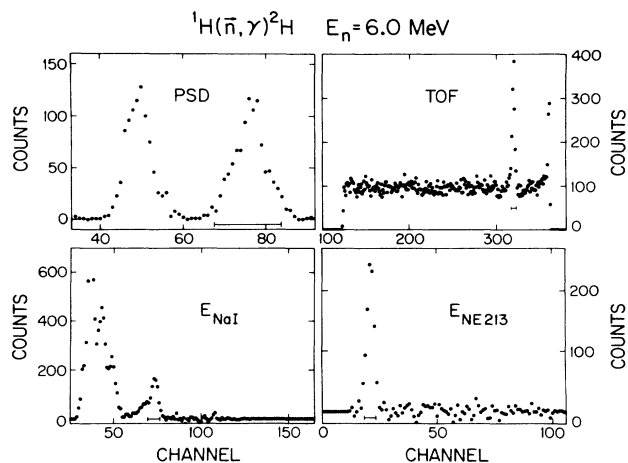


FIG. 4. Typical spectra of real events at $E_n=6.0$ MeV. Each spectrum shows those events which fall inside the windows in the three remaining spectra. Accidental coincidences have been subtracted from the PSD, E_{NaI} , and E_{NE213} spectra. The statistical uncertainties on the data points are consistent with the scatter in these points.

are from n-p scattering, which produces a recoil proton. One expects that the pulse shape for recoil deuterons should differ somewhat from that for protons, and this is found to be the case. In the final spectra, the windows are symmetric on the recoil deuteron peaks.

The spectra obtained with the optimized windows still contain accidental coincidences. The accidentals were removed in the usual way by making use of the flat region in the TOF spectrum.

The final spectra obtained from analysis of the raw data in Figs. 2 and 3 are shown in Figs. 4 and 5. Note that the accidentals have been subtracted from the PSD, E_{NaI} , and E_{NE213} spectra, but are still present in the TOF spectra. The scatter in the points in these spectra (for example, in the region above the peak in the E_{NE213} spectrum at 6 MeV) is consistent with the expected statistical

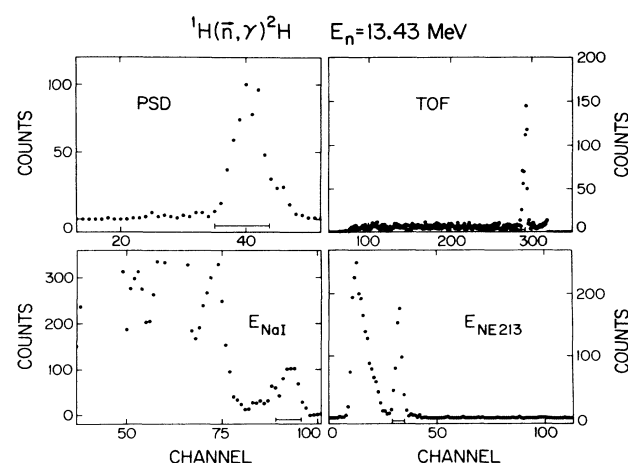


FIG. 5. The same as Fig. 4 at $E_n=13.43$ MeV.

fluctuations. Note that in each spectrum the peak from n-p capture is well separated from other peaks. In the two-dimensional E_{NaI} vs E_{NE213} spectrum, the entire region around the peak of interest is free of background (except for a band which contains the tail from Compton scattering in the NaI detector) once the accidental coincidences have been subtracted. In view of this, we are confident that the peak region does not contain a significant number of counts from processes other than n-p capture.

The observed counting rate after all cuts is reasonably consistent with the known capture cross section, provided that one includes corrections for a variety of processes (neutron and γ -ray attenuation, NaI photopeak efficiency, etc.) that tend to reduce the observed rate. This gives us added confidence that we have correctly identified the n-p capture events.

B. Calculation of the analyzing power

The cross section for polarized n-p capture may be expressed as

$$\sigma^\pm(\theta) = \sigma_0(\theta)[1 + P^\pm A(\theta)], \quad (1)$$

where σ_0 is the unpolarized cross section, A is the reaction analyzing power, and P is the component of the neutron polarization along the direction $\mathbf{k}_n \times \mathbf{k}_\gamma$. Here the superscripts $+$ and $-$ refer to the two polarization states of the incident beam. If we let N be the observed number of n-p capture events for a given run and I be the time-integrated neutron flux on target during the run, then the analyzing power is given by

$$A = \frac{(N^+/I^+) - (N^-/I^-)}{P^+(N^-/I^-) - P^-(N^+/I^+)}. \quad (2)$$

As described above, the integrated neutron flux is proportional to the number of high-energy neutrons observed in the liquid scintillator in coincidence with the IC pulser. Corrections for dead time are unnecessary since the same electronics are used to measure both the peak yield and the integrated charge.

C. Multiple scattering corrections

Since both the target and the NaI crystal are large, one must correct both for finite geometry and for multiple scattering in the target. There are a number of effects which could, in principle, produce a false symmetry in the experiment. For example, the centroid of the neutron flux from the neutron production cell is not along the incident beam direction, since the production reaction has a nonzero analyzing power. Thus, the centroid will be closer to the NaI crystal for one spin state than for the other, resulting in a larger solid angle for the detector. This effect is compounded by the attenuation of the gamma rays in the target. Those gammas which are produced farther from the NaI crystal also have a greater probability of being lost. The combined result of these two effects is that the count rate will be enhanced for one spin state and suppressed for the other.

In addition, one must correct for multiple scattering in

the target. Approximately 40% of the neutrons which strike the target scatter at least once from either hydrogen or carbon. One might therefore expect a large fraction of the detected n-p capture events to result from neutrons which have undergone a previous interaction. If the neutrons scatter through a large angle, or if scattering from hydrogen or carbon has a large analyzing power, these events could produce a false asymmetry.

The magnitudes of these and other effects were estimated by using a Monte Carlo computer code to simulate the experiment. According to these calculations (which are described in detail in Ref. 17), the measured analyzing power should be corrected by an amount

$$\begin{aligned} \Delta A &= -0.0026 \pm 0.0006 \quad \text{at } E_n = 6.0 \text{ MeV}, \\ \Delta A &= +0.0003 \pm 0.0005 \quad \text{at } E_n = 13.43 \text{ MeV}, \end{aligned} \quad (3)$$

where the error quoted represents the statistical uncertainty in the Monte Carlo calculation. The values of ΔA are small compared to the statistical uncertainties in the measurements.

Estimates of the main multiple scattering effects, obtained by carrying out hand calculations which are completely independent of the Monte Carlo program, verify the conclusion that the corrections are on the order of 10^{-3} . The reason that the corrections are so small is that the liquid scintillator and the NaI crystal both have good energy resolution, and this permits us to put tight windows on the energy peaks in our experiment. These windows effectively eliminate most of the events induced by multiply scattered neutrons. While approximately 40% of the neutrons scatter at least once, only about 5% of the events in the real peak involve multiply scattered neutrons.

IV. RESULTS AND CONCLUSIONS

The final measured analyzing powers are given in Table I. These results include the multiple scattering corrections given in Eq. (3). The quoted uncertainties are dominated by the statistical errors in the peak sums, but also include statistical errors in the measurement of the beam polarization and integrated flux, errors associated with the subtraction of accidental coincidences, and the overall normalization uncertainty in the neutron beam polarization. This latter contribution arises in part from the uncertainty in the calibration of the polarimeters ($\pm 2\%$) and in part from the uncertainty in the polarization transfer coefficients^{10,11} ($\pm 5\%$ at 6 MeV and $\pm 2\%$ at 13.43 MeV). Note that both measurements were obtained at $\theta_{\text{lab}} = 90^\circ$ rather than $\theta_{\text{c.m.}} = 90^\circ$. However, the angular dependence of the analyzing power is expected to be flat near 90° (see, for example, Ref. 6) and the resulting error is negligible compared to the statistical uncertainty. The quantity E_γ^{inv}

TABLE I. Final n-p capture analyzing power results.

E_n (MeV)	$\theta_{\text{c.m.}}$ (deg)	E_γ^{inv} (MeV)	A
6.0	93.2	5.24	-0.0681 ± 0.0274
13.43	94.9	9.00	-0.0954 ± 0.0268

in Table I is the gamma ray energy for the corresponding inverse reaction. Each of the two measurements represents about 5 weeks of beam time.

In Fig. 6 we show the results of the present experiment along with previous measurements^{1,3-5} of the outgoing neutron polarization for the inverse reaction. One notes that both of our measurements are reasonably consistent with the overall trend of the previous data.

The curve in Fig. 6 shows the theoretical calculation of Hadjimichael.⁷ This calculation combines classical impulse results similar to those of Partovi⁶ with corrections arising from meson exchange currents (MEC's). It is apparent from Fig. 6 that the agreement between theory and experiment is less than perfect. Most of the measurements lie well above the theoretical curve (only one point out of 16 lies below), and the χ^2 per degree of freedom is significantly greater than one ($\chi^2/N=6.24$).

Although one might conclude at this point that the calculation shown in Fig. 6 is lacking in some respect, one should first consider the possibility that the discrepancy is due to experimental problems. One way to assess the reliability of the experiments is to look at the consistency of the measurements. If we attempt to draw a straight line through the data, the best fit has $\chi^2/N=1.28$. It is apparent in Fig. 6 that the largest contributions to this χ^2 arise from the measurements of Dooks,⁵ which tend to lie somewhat below the trend of the data from the other experiments. If one disregards these measurements the straight line fit improves by a significant amount to $\chi^2/N=0.99$. Thus we see that four of the five experiments represented in Fig. 6 are mutually consistent. Each of these four experiments clearly favors neutron polarizations which are more positive than the theoretical curve.

Although the measurements in Fig. 6 represent several different experiments, nearly all of the data points shown were obtained using essentially the same experimental approach (in which the polarization of the neutrons from

deuteron photodisintegration is determined by elastic scattering from carbon). This is cause for some concern, since it raises the possibility that the various experiments could be subject to some common systematic error. It should be noted, however, that for the data points at $E_\gamma=13.5$ and 14.0 MeV, elastic scattering from helium was used to measure the neutron polarization. It is significant that both of these data points as well as those from the present experiment (for which a completely different experimental approach was used) are consistent with the trend of the other measurements.

In view of these considerations, we think it unlikely that the experiments are in error. One is left with the conclusion that some important ingredient is missing in the theoretical calculations. It should be noted that the use of different nucleon-nucleon potentials does not shift the calculated neutron polarizations enough to resolve the discrepancy (see, for example, Ref. 2).

Holt *et al.*¹ and Rustgi *et al.*² have emphasized the fact that when one includes the MEC contributions, the calculated polarization moves to more negative values, which makes the agreement with the measurements worse. This observation might lead one to conclude that the problem lies with the MEC corrections. However, it is generally believed (see, for example, Ref. 18) that the procedure for introducing meson-exchange corrections is relatively unambiguous for isovector magnetic transitions. Since the exchange corrections for the n-p capture analyzing power involve the $^1S_0 \rightarrow ^3S_1$ transition, we think that the discrepancies are most likely the result of some completely unrelated problem.

Recently, Friar *et al.*¹⁹ have shown that the electromagnetic spin-orbit interaction (which has relativistic origins and is therefore not included in the conventional impulse calculations) can have important effects in deuteron photodisintegration. In particular, they find that including this interaction apparently resolves the long-standing discrepancy between measurements and calculations of the photodisintegration cross section at 0° . On the surface, this interaction appears to be a good candidate for resolving the neutron polarization problem as well, since it depends explicitly on the nucleon spins and is of about the right order of magnitude. However, a detailed investigation of the problem shows that the effect of this interaction is, in fact, quite small. In general, one expects that the largest contributions should arise from interference of the amplitudes which results from the electric dipole part of the spin-orbit interaction with the conventional $E1$ amplitude. However, one finds that the $E1$ interference contribution varies with angle as $\sin\theta \cos\theta$ and thus vanishes at $\theta=90^\circ$. Furthermore, the relative phase of the two $E1$ amplitudes is such that, even for angles away from 90° , the neutron polarization is affected very little.

V. SUMMARY

Measurements of the analyzing power for neutron-proton radiative capture at $\theta=90^\circ$ have been presented for neutron lab energies of 6.0 and 13.43 MeV. By time reversal invariance this is equivalent to measuring the polar-

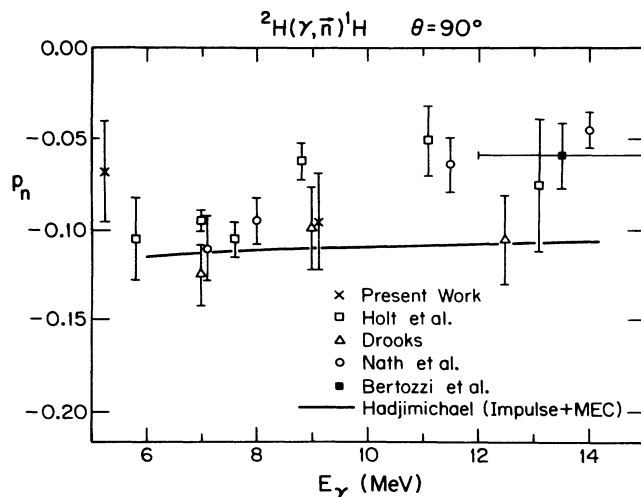


FIG. 6. Polarization of the outgoing neutrons from deuteron photodisintegration at $\theta=90^\circ$ for gamma ray energies between 5 and 15 MeV. The curve shows the calculation of Hadjimichael (Ref. 7), which includes meson exchange corrections.

ization of the outgoing neutrons from deuteron photodisintegration (p_n) at photon energies of 5.24 and 9.0 MeV. If one disregards the results of Drooks,⁵ the remaining measurements of p_n at $\theta_{c.m.} = 90^\circ$ are mutually consistent (see Fig. 6). Present theoretical calculations for deuteron photodisintegration⁷ do not reproduce these measurements accurately.

In view of the fact that deuteron photodisintegration is the simplest of all nuclear reactions, one can hardly overemphasize the importance of resolving this issue and

of developing the theory to the point where one can make reliable predictions of all observables.

ACKNOWLEDGMENTS

The authors would like to thank Dr. Alex Chisholm for his help during the early stages of the experiment. This work was supported in part by a grant from the National Science Foundation.

*Present address: Department of Physics, North Carolina State University, Raleigh, NC 27695.

¹R. J. Holt, K. Stephenson, and J. R. Specht, *Phys. Rev. Lett.* **50**, 577 (1983).

²M. L. Rustgi, Reeta Vyas, and Manoj Chopra, *Phys. Rev. Lett.* **50**, 236 (1983).

³W. Bertozzi, P. T. Demos, S. Kowalski, C. P. Sargent, W. Turchinetz, R. Fullwood, and J. Russell, *Phys. Rev. Lett.* **10**, 106 (1963).

⁴R. Nath, F. W. K. Firk, and H. L. Schultz, *Nucl. Phys.* **A194**, 49 (1972).

⁵L. J. Drooks, Ph.D. thesis, Yale University, 1976; F. W. Firk, in *Proceedings of the International Conference on the Interactions of Neutrons with Nuclei*, Lowell, 1976, edited by E. Sheldon (U.S. Dept. of Commerce, Springfield, Virginia, 1976), p. 389 (available from the National Technical Information Service, U.S. Department of Commerce, Springfield, Virginia 22161).

⁶F. Partovi, *Ann. Phys. (N.Y.)* **27**, 79 (1964).

⁷E. Hadjimichael, *Phys. Lett.* **46B**, 147 (1973).

⁸H. Arenhovel, W. Fabian, and H. G. Miller, *Phys. Lett.* **52B**, 303 (1974).

⁹W. Haeberli, M. D. Barker, C. A. Gossett, D. G. Mavis, P. A.

Quin, J. Sowinski, and T. Wise, *Nucl. Instrum. Methods* **196**, 319 (1982).

¹⁰R. C. Haight, J. E. Simmons, and T. R. Donoghue, *Phys. Rev. C* **5**, 182 (1972).

¹¹P. W. Lisowski, R. L. Walter, C. E. Busch, and T. B. Clegg, *Nucl. Phys.* **A242**, 298 (1975).

¹²M. D. Barker, User's Guide to the Barker Polarimeter, University of Wisconsin, 1982 (unpublished).

¹³K. Stephenson and W. Haeberli, *Nucl. Instrum. Methods* **169**, 483 (1980).

¹⁴M. D. Barker, Ph.D. thesis, University of Wisconsin, 1983, available from University Microfilms International, Ann Arbor, MI 48106.

¹⁵C. A. Gossett, Ph.D. thesis, University of Wisconsin, 1983, available from University Microfilms International, Ann Arbor, MI 48106.

¹⁶C. M. Bartle, *Nucl. Instrum. Methods* **124**, 547 (1975).

¹⁷J. P. Soderstrum, Ph.D. thesis, University of Wisconsin, 1984, available from University Microfilms International, Ann Arbor, MI 48106.

¹⁸J. F. Mathiot, *Nucl. Phys.* **A446**, 123C (1985).

¹⁹J. L. Friar, B. F. Gibson, and G. L. Payne, *Phys. Rev. C* **30**, 441 (1984).